AD-A188 213 DEPOLARIZED INFRARED REFLECTANCE FROM DRY AND WETTED SURFACES(U) CHEMICAL RESEARCH DEVELOPMENT AND ENGINEERING CENTER ABERDEEN.. A H CARRIERI ET AL. 1/1

UNCLASSIFIED SEP 87 CREDC-TR-87084 F/G 20/6 NL

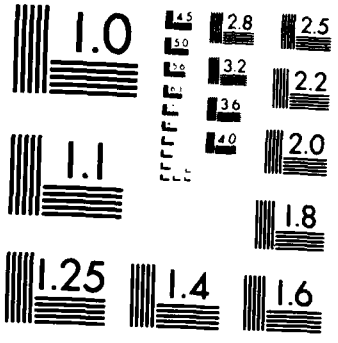

CHEMICAL
RESEARCH,
DEVELOPMENT &
ENGINEERING
CENTER

CRDEC-TR-87084

DEPOLARIZED INFRARED REFLECTANCE FROM DRY AND WETTED SURFACES

by Arthur H. Carrieri
John T. Ditillo
Mark S. Schlein

DETECTION DIRECTORATE

September 1987

U.S. ARMY
ARMAMENT
MUNITIONS
CHEMICAL COMMAND

Aberdeen Proving Ground, Maryland 21010-5423

Disclaimer

The findings in this report are not to be construed as an official Department of the Army position unless so designated by other authorizing documents.

Distribution Statement

Approved for public release; distribution is unlimited.

REPORT DOCUMENTATION PAGE

1a. REPORT SECURITY CLASSIFICATION UNCLASSIFIED	1b RESTRICTIVE MARKINGS
2a. SECURITY CLASSIFICATION AUTHORITY	3 DISTRIBUTION / AVAILABILITY OF REPORT Approved for public release; distribution is unlimited.
2b. DECLASSIFICATION / DOWNGRADING SCHEDULE	
4. PERFORMING ORGANIZATION REPORT NUMBER(S) CRDEC-TR-87084	5 MONITORING ORGANIZATION REPORT NUMBER(S)
6a NAME OF PERFORMING ORGANIZATION CRDEC 6b OFFICE SYMBOL (*If applicable*) SMCCR-DDT	7a. NAME OF MONITORING ORGANIZATION
6c. ADDRESS (*City, State, and ZIP Code*) Aberdeen Proving Ground, MD 21010-5423	7b ADDRESS (*City, State, and ZIP Code*)
8a. NAME OF FUNDING / SPONSORING ORGANIZATION CRDEC 8b. OFFICE SYMBOL (*If applicable*) SMCCR-DDT	9. PROCUREMENT INSTRUMENT IDENTIFICATION NUMBER
8c. ADDRESS (*City, State, and ZIP Code*) Aberdeen Proving Ground, MD 21010-5423	10 SOURCE OF FUNDING NUMBERS PROGRAM ELEMENT NO PROJECT NO 1L161102 TASK NO A71A WORK UNIT ACCESSION NO
11 TITLE (*Include Security Classification*) Depolarized Infrared Reflectance from Dry and Wetted Surfaces	
12 PERSONAL AUTHOR(S) Carrieri, Arthur H., Ditillo, John T., and Schlein, Mark S.	
13a. TYPE OF REPORT Technical 13b. TIME COVERED FROM 85 12 TO 86 11	14 DATE OF REPORT (*Year, Month, Day*) 1987 September 15 PAGE COUNT 24
16 SUPPLEMENTARY NOTATION	

17 COSATI CODES		
FIELD	GROUP	SUB-GROUP
15	06/03	

18. SUBJECT TERMS (*Continue on reverse if necessary and identify by block number*)
Depolarized radiance
Isotropic radiance
Dielectric surface
Light scattering
Detection
Targeted liquid contamination

19 ABSTRACT (*Continue on reverse if necessary and identify by block number*)

Backscattering of the CO_2 laser was measured from soil, sand, concrete, asphalt, and military-specified painted metal plates before and after contamination by an infrared-absorbing liquid. Sensitivity of the 9- to 11-μm volume reflectance spectra to the targeted liquid contamination differed significantly between porous and nonporous scattering surfaces, indicating that diffusion of liquid into the material bulk, not resonant absorption of the probe laser by the liquid, dictates direct detection sensitivity threshold.

20 DISTRIBUTION / AVAILABILITY OF ABSTRACT ☒ UNCLASSIFIED/UNLIMITED ☐ SAME AS RPT ☐ DTIC USERS	21 ABSTRACT SECURITY CLASSIFICATION UNCLASSIFIED
22a NAME OF RESPONSIBLE INDIVIDUAL TIMOTHY E. HAMPTON	22b TELEPHONE (*Include Area Code*) (301) 671-2914 22c OFFICE SYMBOL SMCCR-SPS-T

DD FORM 1473, 84 MAR 83 APR edition may be used until exhausted
All other editions are obsolete

PREFACE

The work described in this report was authorized under Project No. 1L161102A71A, Chemistry and Physics of Surfaces. This work was started in December 1985 and completed in November 1986.

The use of trade names or manufacturers' names in this report does not constitute an official endorsement of any commercial products. This report may not be cited for purposes of advertisement.

This report has been approved for release to the public.

Acknowledgments

The authors gratefully acknowledge the software contributions to this project from our colleague William Loerop. Bill developed the model software and the graphics portions of the code used in our analyses. Author Carrieri is thankful to another colleague, Merrill Milham, for making available the optical constants data from minerals and the subsequent penetration depth calculations.

Blank

CONTENTS

		Page
1.	INTRODUCTION	7
2.	THEORY	8
2.1	Liquid Coating Formed on an Impermeable Volume Scattering Substrate	8
2.2	Liquid Diffused Into the Bulk of a Porous Volume Scatterer	14
3.	EXPERIMENTAL APPROACH	14
4.	RESULTS, DISCUSSION, CONCLUSION, AND FUTURE WORK	18
	LITERATURE CITED	23

Blank

DEPOLARIZED INFRARED REFLECTANCE FROM DRY AND WETTED SURFACES

1. INTRODUCTION

In this study, we incorporated two experimentally verified properties[1] of light scattering to the active, direct detection of a targeted liquid on/within an inhomogeneous dielectric surface. One property is that multiple scattering is a subsurface effect and accounts for depolarized radiance; the other property is that this depolarized component is Lambertian (isotropic radiance) and not correlated to topographical detail of the irradiated surface. The goals of these investigations are to separate and measure volume–scattering powers and to determine the spectral sensitiveness versus applied contamination density. Although volume scattering in the mid infrared (MIR) accounts for only a minor percentage of the total scattering signal from soil, sand, asphalt, and concrete surfaces (these surfaces of interest absorb MIR radiation, and the stronger the absorption the less the volume scattering), we suspect that this component alone contains a greater percentage of information influenced by the liquid and that by being a subsurface effect is insensitive to surface roughness. The work of Renau et al.[1] was extended from the visible wavelength of 0.6328 μm to the 9– to 11–μm band of the MIR, and the dielectric media were contaminated by ejection of a nonvolatile liquid with strong resonant absorption centered about 9.7 μm. As a consequence of the greater wavelengths of our probe beam, the depolarized component makes up only about 10% of the total backscattered light in comparison to about 80% from the scattering of a He–Ne beam by soil particles, for instance. The liquid lying on and/or diffused through the surface is targeted by its ability to absorb in the MIR band. Selective absorption is the basis for discriminating against the target by irradiating the contaminated surface at alternate wavelengths centered on and off the absorption

peak of the liquid (laser line bandwidth << liquid absorption bandwidth) and analyzing the difference in backscattered signals. After filtering out the reflectance spectral response of the unwetted surface, a condition can be defined that will cause an alarm to trip, for instance, based on the magnitude in the difference signals, indicating the probability of an absorption match between sample and target.

2. THEORY

2.1 *Liquid Coating Formed on an Impermeable Volume Scattering Substrate.*

A restrictive class of contaminated surfaces are those that will retain dispersed liquid droplets on their surface. A metal plate with military–specified primer coating and paint layer, which was used in these experiments, is such a surface. After striking the paint layer, the droplets spread and eventually form a thin film. The method for detecting this liquid layer is shown in Figure 1. A linearly polarized incident beam generates a source of volume–backscattered radiance that back–transmits through the liquid layer. The volume reflectance signature will therefore maximize/minimize at wavelengths that are nonabsorbing/absorbing by the liquid. This differential reflectance feature contains quantitative (possible density mapping applications) as well as qualitative (detection) information, since the depolarized reflectance component is related to film thickness (Equation 3b) via amplitude attenuation of the multiple–scattered waves transmitting through the liquid layer at wavelengths where refractive index in the liquid is complex ($k \neq 0$).

Depolarized Reflectance Modeling Equations.

From specular reflection properties of the liquid layer[2] and radiometric definitions of radiance and irradiance,[3] a volume reflectance function that solves the

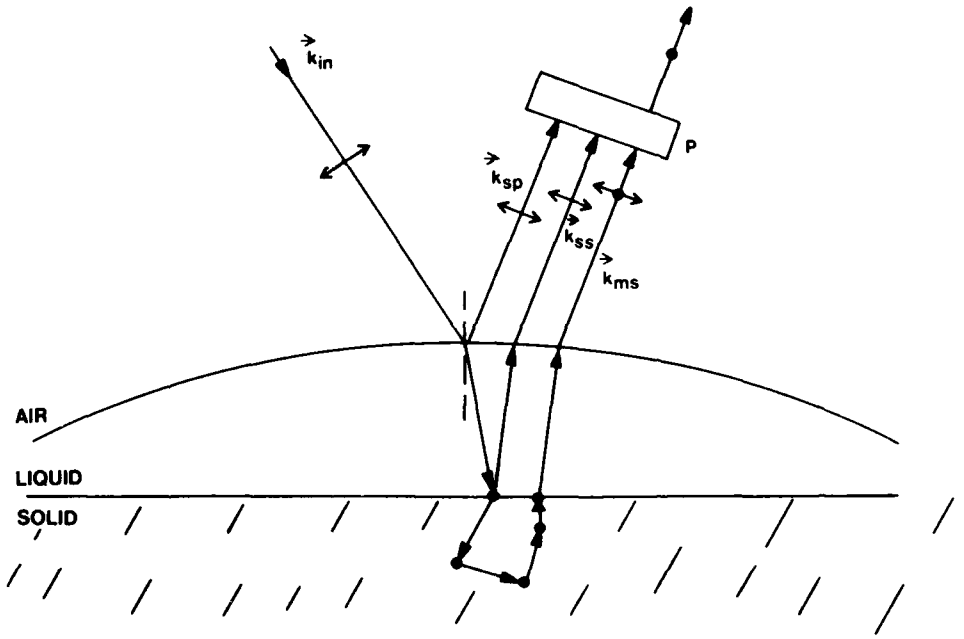

FIGURE 1. The proposed concept for direct detection of an IR absorbing liquid on an impermeable dielectric surface. $\vec{k}_{in}$, $\vec{k}_{sp}$, $\vec{k}_{ss}$ and $\vec{k}_{ms}$ are wave vectors of the incident parallel-polarized wave; the specularly reflected parallel-polarized wave; a modified single-scattered parallel-polarized wave; and a modified multiple-scattered polarization-shifted wave, respectively. P is a polarizer with transmission axis perpendicular to the plane of incidence.

boundary value problem depicted in Figure 1 was obtained and is given below. This solution is a variation of the model given in Wolfe and Zissis' handbook[4] rederived by Rosengreen and coworkers[5] and is nonrigorous (ρ_v is an experimental input) with the assumption of *a priori* Lambertian volume reflectance from the unwetted surface. The model, however limited in usefulness, can provide relative reflectance differences as modified by varying layers of the absorbing film. The selection of wavelengths that most discriminate against the contaminant is thereby simplified. Volume reflectance defined as the ratio of depolarized radiant power transmitted through the liquid layer to total incident beam power (Figure 1) is given by:

$$f_v = \rho_v \frac{(1-\rho_s)\tau(1-\tilde{\rho}_s)\tilde{\tau}}{1-\rho_v\left(\int_{\Omega_h}\tilde{\tau}d\Omega_h\right)^2\tilde{\rho}_s/\pi} \tag{1}$$

where;

ρ_v *denotes volume reflectance of the unwetted sample*,

ρ_s *denotes specular reflection of the incident beam at the air−to−liquid interface*,

$$\rho_s = \begin{cases} \dfrac{[\cos^2\theta_i-(n^2+k^2)\cos^2\theta_t]^2+4k^2\cos^2\theta_t\cos^2\theta_i}{[(n\cos\theta_i+\cos\theta_t)^2+k^2\cos^2\theta_i]^2} & \vec{E}\perp \\ \dfrac{[(k^2+n^2)\cos^2\theta_i-\cos^2\theta_t]^2+4k^2\cos^2\theta_t\cos^2\theta_i}{[(n\cos\theta_i+\cos\theta_t)^2+k^2\cos^2\theta_i]^2} & \vec{E}\parallel \end{cases} \quad \textit{plane of incidence.} \tag{2}$$

τ and $\tilde{\tau}$ *are transmission functions given by*:

$$\tau(\theta_i) = e^{-\frac{\beta}{\cos\theta_i}}, \tag{3a}$$

$$\tilde{\tau}(\Theta_i) = e^{-\frac{\beta}{\cos\Theta_i}}, \tag{3b}$$

and

$$\beta \equiv \frac{4\pi wk(\lambda)}{\lambda}.$$

$\tilde{\rho}_s$ denotes reflectance of depolarized radiance at the liquid−to−air interface,

$\tilde{\rho}_s =$

$$\frac{\int_0^{\sin\Theta_c} \tilde{\tau}(\Theta_i)[\rho_{per}(\Theta_i,\Theta_t;\lambda)+\rho_{par}(\Theta_i,\Theta_t;\lambda)]\sin\Theta_i d\sin\Theta_i + 2\int_{\sin\Theta_c}^{1} \tilde{\tau}(\Theta_i)\sin\Theta_i d\sin\Theta_i}{\int_0^1 \tilde{\tau}(\Theta_i)\sin\Theta_i d\sin\Theta_i} \tag{4a}$$

$$2\int_{\sin\Theta_c}^{1} \tilde{\tau}(\Theta_i)\sin(\Theta_i) d\sin\Theta_i = \frac{e^{-\beta sec\,\Theta_c}}{sec^2\Theta_c}(1-\beta sec\,\Theta_c) - \beta^2 Ei(-\beta sec\,\Theta_c) \tag{4b}$$

where;

w is thickness of the liquid layer,

$n(\lambda)$ and $k(\lambda)$ donote real and imaginary parts of the

liquids' complex refractive index,

θ_i, θ_t *are incident, transmitted beam angles at the air−to−liquid interface ,*

Θ_i, Θ_t and Θ_c *are incident, transmitted* and *critical ray angles*

at the liquid−to−air interface,

(all angles are measured relative the liquid surface normal)

and E_i *is the Exponential−Integral function.* [6,*]

A wavefront propagating within the liquid medium at wavelengths where $k \neq 0$ is 'inhomogeneous' by nature, viz, its surfaces of constant phase and constant amplitude do not generally coincide. This implies a complex interpretation of Snell's law and further implies that the propagation direction of a plane wave refracted into the *absorbing* liquid layer is given by:[7]

$$\cos\theta_t = \frac{q(n\cos\gamma - k\sin\gamma)}{\sqrt{\sin^2\theta_i + q^2(n\cos\gamma - k\sin\gamma)^2}} \tag{5a}$$

where;

$$q^2(\theta_i) \equiv \sqrt{(1 - A\sin^2\theta_i)^2 + (B\sin^2\theta_i)^2}, \tag{5b}$$

$$B \equiv \frac{2(k/n)}{n^2[1+(k/n)^2]^2}, \tag{5c}$$

$$A \equiv \frac{n^2 - k^2}{(n^2+k^2)^2}, \tag{5d}$$

* Intergal 3.351 applies to Equation 4a when substituting $y \equiv (\cos\Theta_i)^{-1}$. See section 8.2 for properties of the exponential−integral function.

$$\gamma(\theta_i) \equiv \tfrac{1}{2}\tan^{-1}\left\{\frac{B\sin^2\theta_i}{1-A\sin^2\theta_i}\right\}, \tag{5e}$$

and like expressions for a polarization–shifted, volume–scattered ray inside the liquid propagating toward and refracted at the liquid–to–air interface. Note that Equation 5a reduces to the more recognizable $\sin\theta_i = n\sin\theta_t$ Snell law when k=0.

The perpendicular and parallel components of specular reflectivity at the liquid–to–air interface, ρ_{per} and ρ_{par} in Equation 4a, are obtained by replacing (θ_i,θ_t) with (Θ_t,Θ_i) in Equation 2, and the critical angle Θ_c is determined through substitution of $(\Theta_c,\Theta_t = \pi/2)$ for (θ_t,θ_i) in Equations 5a–e. To evaluate Equation 4a, a substitution of variable via Snells' transformation: $\Theta_i \rightarrow g(\Theta_t,n,k)$; $d\sin\Theta_i \rightarrow h(\Theta_t,n,k)d\Theta_t$, was required. The resulting lengthy expression for $\tilde{\rho}_s$ is numerically integrated by a Simpson's rule subroutine in the model code.

The $(1-\rho_s)\tau$ term from Equation 1 is a measure of how much energy is available for volume scattering, while the $\rho_v(1-\tilde{\rho}_s)\tilde{\tau}$ term gauges how much of that energy transmits the liquid layer and is subsequently available for detection. The denominator of Equation 1 results from an infinite number of internal reflections within the smooth, continuous liquid layer, and by applying the binomial expansion: $(1-x)^{-1} = \sum_{i=0}^{\infty} x^i$, *where* $x \equiv \rho_v(\int_{\Omega_h}\tilde{\tau}d\Omega_h)^2\tilde{\rho}_s/\pi \ll 1$.

All the ingredients for evaluating Equation 1 from input parameters λ, $n(\lambda)$ and $k(\lambda)$, $\rho_v(\lambda)$, θ_i, Θ_t, and liquid thickness w are now provided. The modeling software produces three dimensional graphics for generating surfaces of $f_v(\lambda,w)$. An $f_v(\lambda,w=w_0)$ cross section of the computer generated surface can be compared to experimental data from the contaminated surface. Detection is

probable, and film thickness (w_0) is extracted provided a spectral match condition can be established.

2.2 *Liquid Diffused Into the Bulk of a Porous Volume Scatterer.*

A nonvolatile aerosol simulant (i.e., a liquid with rheological and optical properties that approximate a toxic agent compound and is nonchemically reactive with the scattering particles) ejected onto terrains will generally diffuse into a solid bulk with little or no surface retention. The interstitial structure of liquid–coated particles and voids constitute a chemically complex scattering medium to which a true, tested, rigorous statistical reflectance theory does not exist to our knowledge. We do not offer solutions to this problem, but do suggest that the effective medium, extended effective medium, and multiple scattering theories of Bohren and Huffman,[8] Chylek and Srivastava,[9] Stroud and Pan,[9] and Veradan et al.[10] are useful for future modeling work. Before invoking the effective medium theories, however, one must be aware of their constraints, assumptions, and limitations.[11] We finally note that work by Bahar,[12,13,14,15] using a 'Unified Full Wave' approach for solving problems of scattering by nonuniform stratified media, is currently ongoing under contract with CRDEC, and this may provide insight into the problem of the permeable contaminated surfaces.

3. EXPERIMENTAL APPROACH

The optical arrangement, feedback control, data acquisition and processing electronics of the experiment are schematically drawn in Figure 2. SF96,* a nontoxic silicon–based oil, with double–peaked resonant absorption profile between 9 and 11 μm, Figure 3, served as the contaminant and target. A CO_2 waveguide

* SF96 is a simulant of chemical agent VX widely used in military research.

cw laser, grating tunable from its two P− and R−branch vibrational−rotational transitions, provides a selection of 75 wavelengths between 9− and 11−μm, emissions within the MIR window of atmospheric transmission. The CO_2 beam is polarized parallel to the sample plane, with an extinction ratio better than 100:1, and expanded to produce an elliptical cross−sectional area of 6.2 sq cm for a fixed 50 degree angle of incidence. Speckle interference is integrated through beam expansion and by rotating the sample at 1 Hz. Scattered radiance is directed to the detector through a three−mirrored goniometer arm that scans the polar angle in the plane of incidence across the upper hemisphere. The light−receiving system consists of a liquid−nitrogen−cooled, 1 mm x 1 mm HgCdTe photoconductive detector with an AC coupled preamplifier of 375 KHz bandwidth and a detectivity of 1.8×10^{10} $cmHz^{1/2}/watt$, an instantaneous field of view of 0.063 rad, and numerical aperture of 1.59. Incident beam power was fixed at nearly 1 watt after tuning between laser lines (via variable ND filter) so as not to exceed the detector's dynamic range. Given these system parameters and a typical volume reflectance of 10^{-3}, the maximum range for noise−limited signal detection was computed to be 100 meters.[16] Polarization states of scattered light were ascertained by insertion of a quarter−wave plate before the polarizer and appropriate adjustment of each optic's axes.[17] Contaminant and target SF96 was quantitatively dispersed to the test surfaces through an ultrasonic nebulizing nozzle contained inside a pneumatic chamber. Software was written to control rotation of the Ge polarizer's optical axis and extract minimum and maximum detector voltages for each wavelength in measurement sequence of reference, dry, and wet samples.[18] The depolarized reflectance component is proportional to the ratio of this minimum signal of scattered radiance to the voltage generated by the incident split beam striking a pyroelectric detector. These ratioed voltages were further ratioed to reflectance from a standard Lambertian reflector, with properties of spectral flatness between 9

and 11 μm and diffuse reflectance comparable to the sample. ('Flowers of sulfur' powder is a common standard used in IR spectroscopy.) Absolute reflectance is obtained from a separate experiment by referencing the standard reflector to a known gold reflector.

4. RESULTS, DISCUSSION, CONCLUSION, AND FUTURE WORK

Scattering by all but one surface produced a combination of linear and depolarized components. The exception was a laboratory–grade powdered sulfur sample that produced depolarized and elliptically polarized components because of birefringence in the sulfur crystals. This powder was originally intended, but later rejected, for use as a standard reflector. The polar angle dependence of volume scattering satisfied the $\cos\theta$ Lambertian condition from all measured dry surfaces without exception. By experiment, we attempted to establish the relationship of volume reflectance with the ratio of particle size of a dielectric scatterer to wavelength of the incident beam. The experimental results have shown that the depolarized power component increased by a factor of $\approx$3 between dry alumina crystals, with particle size distributions centered at λ and $\lambda/5$, and by a factor of $\approx$40 between λ and $\lambda/25$ crystals. In general, depolarized power backscattered from all irradiated dry materials prepared for these experiments exhibited spectral dependencies $\sim \lambda^{-n}$. Paint and soil samples (Figures 4a and 5a, dry data), for instance, have shown Rayleigh–like scattering behavior, where n was calculated by least– squares analyses to be 4.3 and 4.5, respectively.

Distinct MIR spectral differences between dry and SF96–sprayed impermeable paint samples were observed to densities of the contaminant as low as 2 gm/M^2, as illustrated by the typical measurement graphed in Figures 4a,b. From the limited reflectance data sets measured from dry and wetted soil, sand, concrete, and asphalt samples, we generally conclude that the spectral response of the

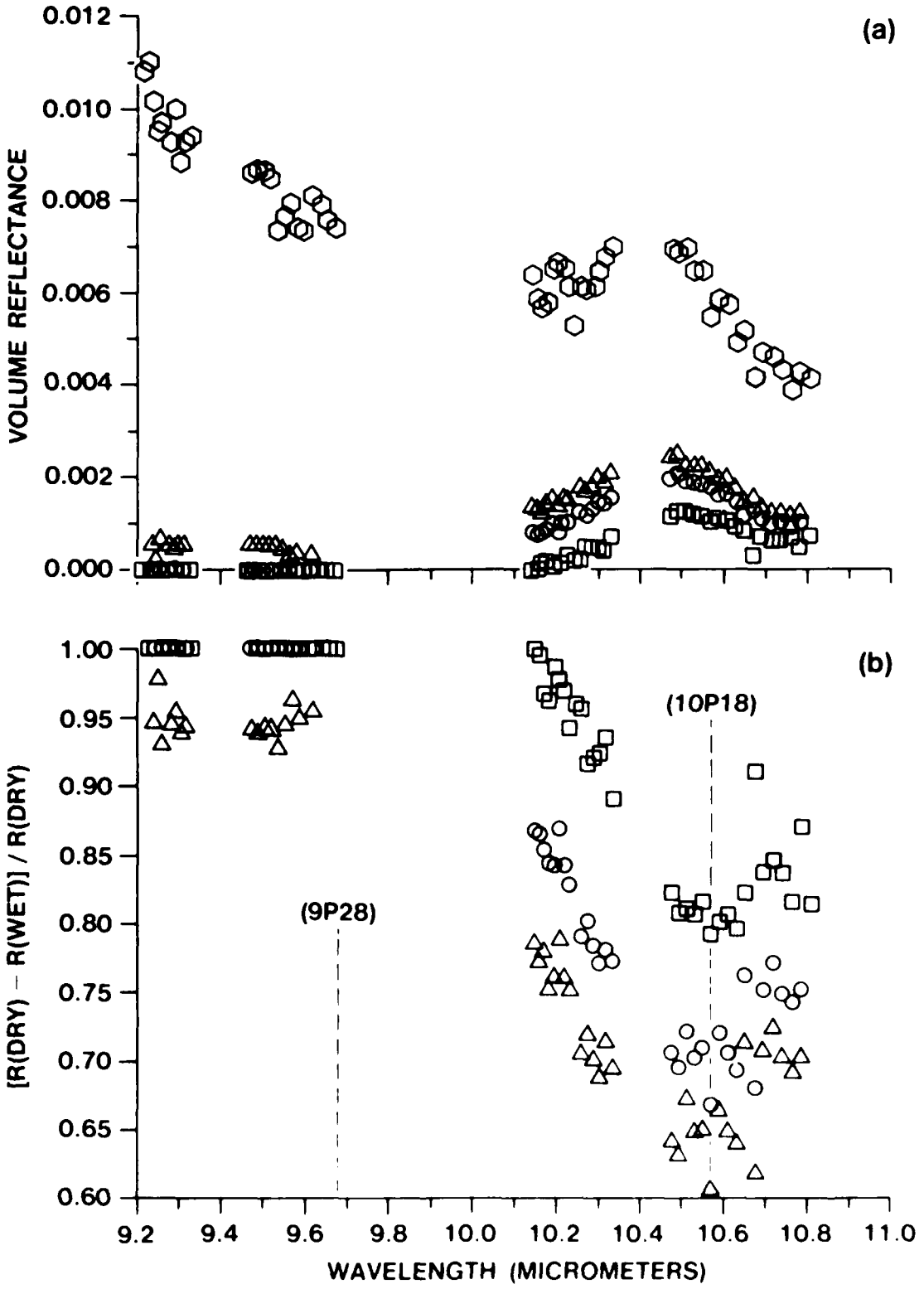

FIGURE 4. Volume reflectance (a) and corresponding difference (b) spectra between a dry (○) and SF96-wetted metallic slab with IR primer and paint layers. The densities of dispersed contamination are: 10 (□), 5 (○), 2 (△) gm/M^2. An analytical (9P28,9.621μ) and reference (10P18,10.571μ) set of probe emissions are indicated in Figure b.

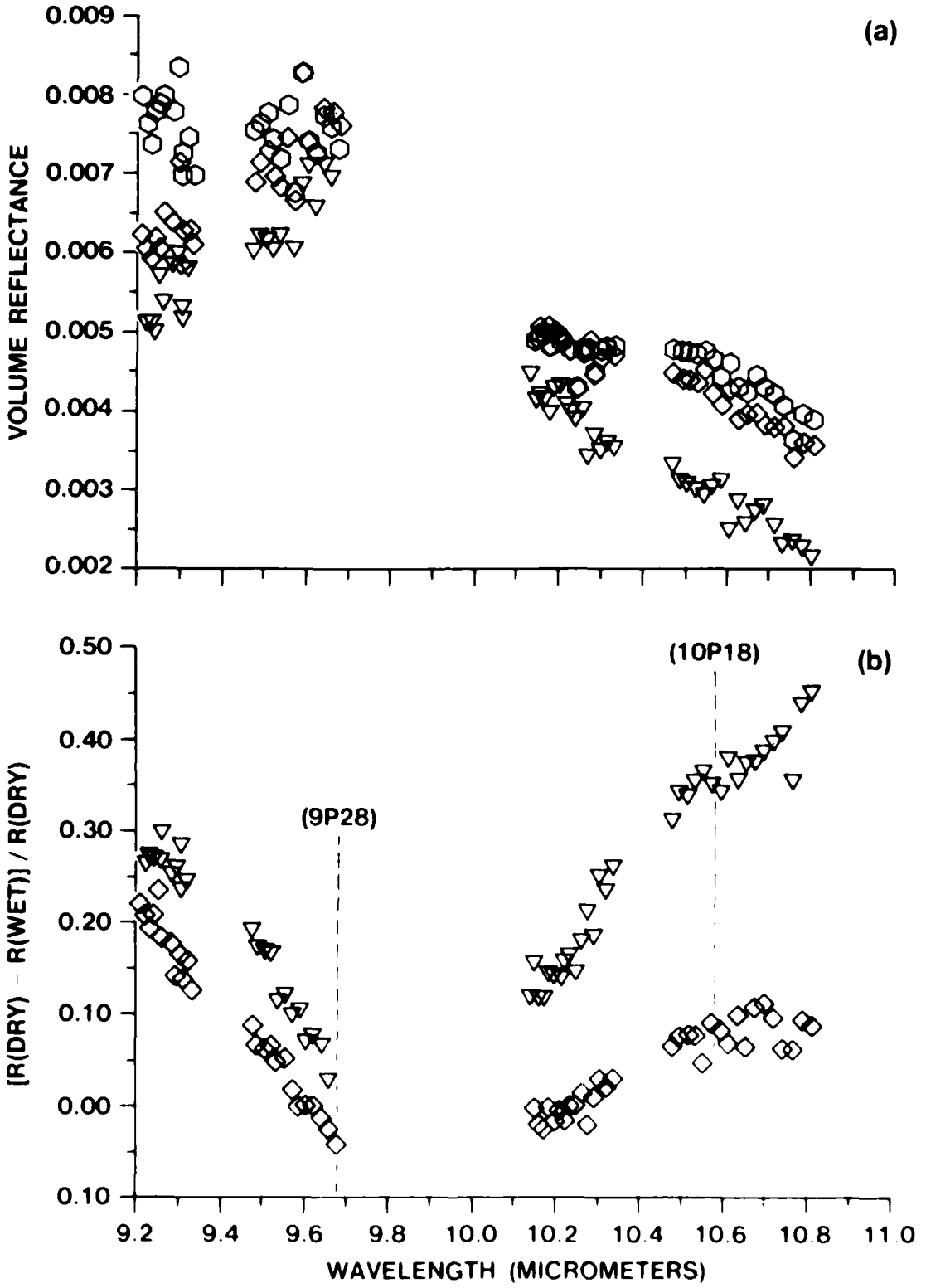

FIGURE 5. Volume reflectance (a) and corresponding difference (b) spectra between dry (○) and SF96-wetted soil samples contaminated to densities of 50 (◇) and 100 (▽) gm/M^2. An analytical (10P18,10.571μ) and reference (9P28,9.621μ) set of probe emissions are indicated in Figure b.

depolarized reflectance component from permeable nonhomogeneous dielectric materials is less sensitive to the SF96 target by at least an order of magnitude of liquid mass. As an example, our results for dry and contaminated soil are shown in Figures 5a,b.

The f_p model code developed for the liquid-coated surface, Figure 1, was applied and compared to the experimental results in Figure 4a. The 3 dimensional graphics output was successful at predicting the extremum located at 10.57 μm and how thick an SF96 film was formed after aerosol ejection onto the painted metal surface. MIR absorption through the film layer is apparent from these data to a contamination density of 2 gm/M^2, perhaps slightly less. Although this may seem encouraging, no claim is made that the data can uniquely determine the contamination; namely, the probability of false alarming can be minimized or eliminated. Indeed, it is not unique since nonvolatile liquids with overlapping absorption bandheads (active detection on/within surfaces must successfully target a class of organophosphonate contaminants, high molecular weight liquids that generally exhibit broad MIR absorption bands) can produce inseparable differential reflectance signatures. As previously mentioned, the contaminated porous surfaces are theoretically difficult to model and experimentally much less spectrally sensitive to the diffused contaminant. A constraint imposed on sensing the diffused liquid within the bulk of impermeable terrains using differential volume scattering is the depth to which the probe beam can penetrate the surface and thereby interact with the liquid cells. Recall, this is one reason volume scattering was separated and chosen as a feature for discrimination. From optical constants data[19,*] of montmorillonite, kaolinite and illite compressed slabs, basic minerals composing soil, a penetration depth at the e^{-2} point minimizes, unfortunately, to about 1 μm, between wavelengths of 9 and 10 μm.

* Private communication with Merrill E. Milham 1986

Mid infrared volume reflectance from dry inhomogeneous dielectric materials was found to be isotropic and inversely dependent on wavelength to some power. This depolarization component's sensitivity to an MIR–absorbing liquid diffused through porous surfaces is limited; the lower limit $\approx$ 20 gm/M^2 SF96 sprayed onto terrains. For an impermeable surface boundary, however, the data suggests that SF96 absorbency can be revealed at densities as low as 2 gm/M^2 (a 2 μm film). These findings may spur continuing efforts on direct detection methods to improve sensitivity, however, new technologies which are more sensitive to and more fully characterize the scattering surface must be explored to fulfill the Army's remote sensing mission. Current and future experiments in this and other laboratories involve exploration of other light scattering technologies that may provide greater sensitivity and precision (some toxic liquids of interest and their nontoxic derivatives do exhibit overlapping absorption bandheads between 8 - 12 μm) in discriminating against surfaces targeted for known hazardous contaminants. Current work by one of us (Carrieri) is directed toward measurement and analysis of all 16 elements of the Mueller matrix, the 4 x 4 transformation between incident and backscattered Stokes vectors that fully characterizes the scattering surface as functions of scattering angle, contamination density, and wavelength between the 9 - 12.5 μm $^{12}C^{16}O_2$, $^{12}C^{18}O_2$, and $^{14}C^{16}O_2$ laser emission bandwidth.

LITERATURE CITED

1. Renau, J., Cheo, P., and Cooper, H. Depolarization of Linearly Polarized EM Waves Backscattered from Rough Metals and Inhomogeneous Dielectrics. J. Opt. Soc. Am. 57, 4 (1967).

2. Jackson, J.D. Classical Electrodynamics. Second Edition. Chapter 7, pp 278–282. John Wiley and Sons, Inc., New York, NY. 1975.

3. Nicodemus, F.E., et al., National Bureau of Standards Report Number NBS MN–160. Geometric Considerations and Nomenclature for Reflectance. October 1977.

4. Wolfe, W.L., and Zissis, G.L. The Infrared Handbook. Section 3.7. 1978.

5. Rosengreen, A. et al., Studies of DIAL/DISC Remote Sensing: Reflectance from VX–Contaminated Surfaces and Development of a Reflectance Model. U.S. Army Contract Number DAAK11–79–C–0084. SRI International. Menlo Park, California. (June 1983)

6. Gradshteyn, I.S., and Ryzhik, I.M. Table of Integrals, Series and Products. Academic Press, New York, NY. 1980.

7. Born, M. and Wolf, E. Principles of Optics. Fifth Edition, Chapter 13. Pergamon Press, New York, NY. 1975.

8. Bohren, C. and Huffman, D. Absorption and Scattering of Light by Small Particles. John Wiley and Sons, Inc., New York, NY. 1983.

9. Chylek, P., and Srivastava, V. Dielectric Constant of a Composite Inhomogeneous Medium. Phys. Rev. B27, 5098 5109 (1983).

Stroud, D. and Pan, F.P. Self Consistent Approach to Electromagnetic Wave Propagation in Composite Media: Application to Model Granular Metals. Phys. Rev. B17, 1602 1610 (1978).

10. Varadan, V.K, Bringi, V.N, Varadan, V.V., and Ishimaru, A. Multiple Scattering Theory of Dielectric Media. Radio Sci. 18, 321 327 (1983).

11. Bohren, C.F. Applicability of Effective Medium Theories to Problems of Scattering and Absorption by Nonhomogeneous Atmospheric Particles. J. Atmos. Sci. 43(5), 468–475 (1986).

12. Bahar, E. Full Wave Solutions for Electromagnetic Scattering and Depolarization in Irregular Stratified Media. Radio Sci. 21(4), 543–550 (1986).

13. Bahar, E., and Fritzwater, M. Multiple Scattering by Conducting Particles with Random Rough Surfaces at Infrared and Optical Frequencies. Radio Sci. 21(4), 689–706 (1986).

14. Bahar, E., Chakrabarti, S., and Fritzwater, M. Extinction Cross Sections and Albedos for Particles with Very Rough Surfaces. Appl. Opt. 25, 2530–2536 (1986).

15. Bahar, E., and Fritzwater, M. Scattering and Depolarization of Linearly Polarized Waves by Finitely Conducting Particles of Irregular Shape. J. Appl. Phys. 60(6), 2123–2132 (1986).

16. Hudson, R., Jr., Infrared System Engineering. Eq. 13–12. John Wiley and Sons. New York, NY. 1969.

17. Jenkins F., and White, H. Fundamentals of Optics. Third Edition. Table 27–I, p 562. McGraw–Hill Book Company, New York, NY. 1957.

18. Duggin, M., and Philipson, W. Field Measurement of Reflectance: Some Major Considerations. Appl. Opt. 21, 15 (1982).

19. Querry, M.R. Optical Properties of Natural Minerals and Other Materials in the 350–50,000 cm^{-1} Spectral Region. Unclassified Report Number ARO 16512.2–GS, University of Missouri at Kansas City, Department of Physics. (July 1979 – December 1982)

END

FILMED

FEB. 1988

DTIC